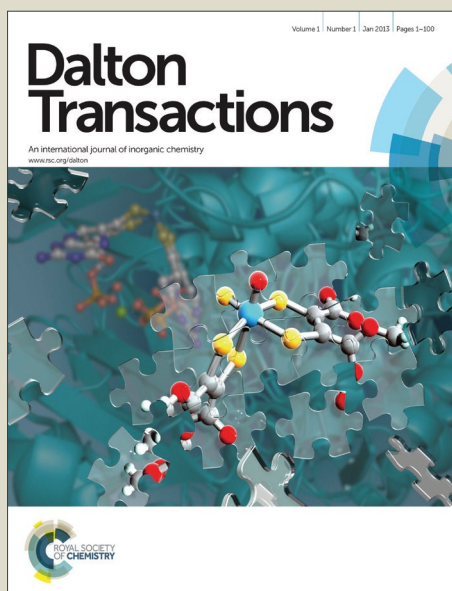


Dalton Transactions

Accepted Manuscript



This article can be cited before page numbers have been issued, to do this please use: M. R. Anneser, S. Haslinger, A. Pöthig, M. Cokoja, V. D'Elia, M. Hogerl, J. Basset and F. E. Kühn, *Dalton Trans.*, 2016, DOI: 10.1039/C6DT00538A.



This is an *Accepted Manuscript*, which has been through the Royal Society of Chemistry peer review process and has been accepted for publication.

Accepted Manuscripts are published online shortly after acceptance, before technical editing, formatting and proof reading. Using this free service, authors can make their results available to the community, in citable form, before we publish the edited article. We will replace this *Accepted Manuscript* with the edited and formatted *Advance Article* as soon as it is available.

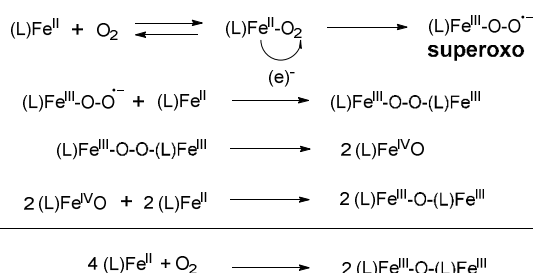
You can find more information about *Accepted Manuscripts* in the [Information for Authors](#).

Please note that technical editing may introduce minor changes to the text and/or graphics, which may alter content. The journal's standard [Terms & Conditions](#) and the [Ethical guidelines](#) still apply. In no event shall the Royal Society of Chemistry be held responsible for any errors or omissions in this *Accepted Manuscript* or any consequences arising from the use of any information it contains.

Results and Discussion

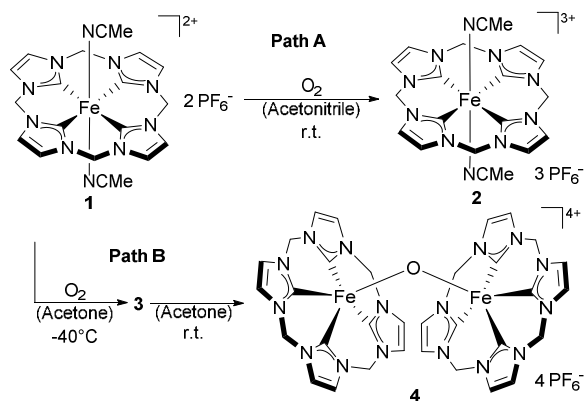
Preliminary observations and UV-Vis spectroscopy studies:

The reactivity of Fe complexes with dioxygen has been previously studied. The reaction leads to dimeric Fe(III)-O-Fe(III) species according with the mechanism presented in Scheme 1.¹⁰



Scheme 1. Stepwise oxidation of an Fe(II) complex to a dimeric Fe(III)-O-Fe(III) species by molecular oxygen.

The formation of a tetra NHC ligated FeOFe complex with oxygen in acetonitrile was reported by Meyer et al.¹¹ In spite of very similar structural features between **1** and the "Meyer-system", the reaction of **1** with oxygen in acetonitrile did not yield the expected FeOFe complex. In this case, oxygen-free species **2** was irreversibly formed and isolated. (Scheme 2, Path A) **2** was reported previously, but its preparation was achieved by oxidation of **1** with stoichiometric amounts of thianthrenyl hexafluorophosphate.⁸ In spite of the absence of a Fe-O bond in **2**, the transformation of **1** to **2** was found to proceed with the intake of nearly 1 equiv. O₂, being indicative for a stoichiometric reaction of **1** and O₂ (see in the ESI, Section 6). Accordingly, the process of formation of **2** from **1** in acetonitrile without observable formation of a FeOFe dimer, is analogous to the oxidation of hemoglobin (Fe^{II}) by O₂ to afford methemoglobin (Fe^{III}) and a superoxide.¹² The reaction of **1** with O₂ (1 bar) in acetonitrile to afford compound **2** was accompanied by a shift in the maximum UV/Vis absorption from 337 nm to 505 nm (Figure 1, see also Figure S1). The prominent absorption of **1** at 337 nm, disappears in the presence of molecular oxygen. Simultaneously, a broad absorption band forms at 505 nm. This band can be assigned to an Fe(III)-NHC LMCT transition.¹³ The broad shape of the absorption is very similar to that reported by Meyer, Kühn et al. for the oxidized Fe(II)-tetracarbene,¹³ though it is slightly blue shifted ($\lambda_{\text{max}} = 505$ nm for **2** versus $\lambda_{\text{max}} = 540$ nm). At 1 bar O₂, the oxidation of **1** by molecular oxygen in acetonitrile is a slow process that could be monitored by UV/Vis spectroscopy (Figure 1); the complete conversion of **1** to **2** was observed within 5 hours at room temperature. The relatively low reaction rate under these conditions could be due to the competing coordination of either acetonitrile or oxygen at the Fe(II) center.



Scheme 2. Divergent oxidation behaviour of **1** in acetone and in acetonitrile leading to complexes **3**, **4** and **2** respectively.

This hypothesis is corroborated by the observation that in the presence of DMSO (10% v/v) no formation of **2** or **3** is detected under ambient conditions. Instead, the formation of a stable DMSO-substituted derivative of **1** is observed.⁷ Moreover, the amount of complex **2** forming within 1 h by the reaction with O₂ increases with the partial O₂ pressure (see in the ESI, Section 7). Taken together these findings indicate that the key step in the oxidation of **1** to **2** is an oxygen-axial ligand exchange that is hampered by axial ligand coordination (MeCN, DMSO, etc.). The overall process is assumed to proceed with the initial displacement of one of the acetonitrile ligands in the axial position and with the formation of a superoxo Fe^{III}-O₂ adduct complex or of a dimeric Fe^{III}-O-O-Fe^{III} species. The fate of the (presumably) formed superoxide or peroxide anion upon formation of **2** is not clear as no additional products of oxidation could be found in solution. One plausible reaction pathway might involve a non-innocent role of the solvent. It is known that acetonitrile can be oxidized to glycolonitrile by molecular oxygen in the presence of Fe^{III}-O-O-Fe^{III} complexes. The reaction has been proposed to proceed via α -proton abstraction by the superbasic peroxy-complex and formation of a cyanomethide intermediate.¹⁴

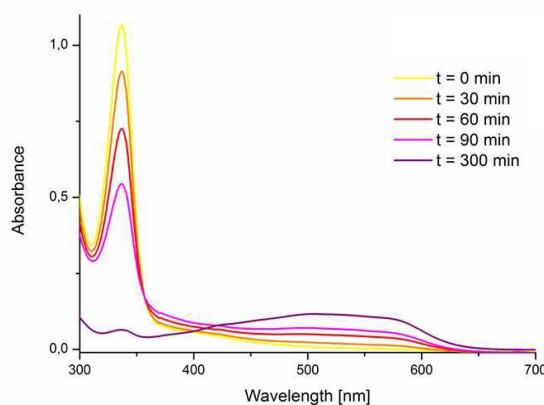


Figure 1. UV/Vis kinetics of the formation of **2** from **1** (initial concentration $2 \cdot 10^{-4}$ M) and O₂ in acetonitrile (r.t., 1 bar). **1** ($\lambda_{\text{max}} = 337$ nm; $\epsilon_{337} = 5450$ l/mol·cm); **2** ($\lambda_{\text{max}} = 505$ nm; $\epsilon_{505} = 1100$ l/mol·cm).

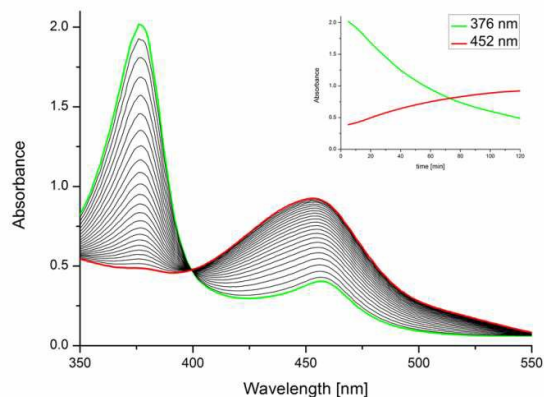


Figure 2. UV/Vis kinetics of the formation of **3** from **1** and O_2 in acetone, sampled every 5 min for 2 h. ($[1]_0 = 4 \cdot 10^{-4}$ M at -20°C , 1 bar O_2). **1**, ($\lambda_{\text{max}} = 376$ nm; $\epsilon_{376} = 5400$ l/mol \cdot cm); **3**, ($\lambda_{\text{max}} = 452$ nm; $\epsilon_{452} = 2700$ l/mol \cdot cm). Insert: time dependent trace of the absorptions at 376 and 452 nm.

Indeed, when different nitriles such as benzonitrile or pivalonitrile, are used as solvents for the reaction of **1** and O_2 , the formation of Fe(III)-O-Fe(III) complex dimer **4** (Scheme 2) was observed instead of **2**. This indicates that in the absence of an abstractable α -proton at the nitrile moiety the reaction between **1** and dioxygen proceeds along the path displayed in scheme 1. Furthermore, it is known that the metabolism of acetonitrile by the Fe-containing enzyme sMMO leads to the formation of cyanide via glycolonitrile as an intermediate.¹⁵ Therefore, the formation and rapid decomposition of chemically unstable glycolonitrile¹⁶ to afford minute amounts of gaseous products might explain the absence of additional oxygenated products detectable in solution upon formation of **2** in acetonitrile. Further observations on the reactivity of isolated superoxide **3** with acetonitrile (*vide infra*) seem to support this hypothesis. In acetone, a different reactivity pattern (scheme 2, Path B) was observed leading to dimeric complex **4**. This pathway proceeds possibly through the mechanism depicted in scheme 1. The formation of Fe(III)-O-Fe(III) dimers from Fe(II) and molecular oxygen is well known for both heme and non-heme iron compounds.¹⁰ Interestingly, when the reaction of **1** with O_2 is carried out at low temperatures in acetone an intermediate compound was

observed by UV/Vis spectroscopy (Figure 2). The formation of the new species from **1** at -20°C is accompanied by the rise of a single absorption in the UV/Vis spectrum at 452 nm and by the disappearance of the absorption of **1** at 376 nm (Figure 2). This compound was proposedly identified as the Fe(O_2) species **3** (Scheme 2) based on EPR and ^1H NMR spectroscopies, reactivity studies and theoretical calculations (*vide infra*). When the solution of **3** is allowed to warm up, dimeric complex **4** is formed. At 0°C , the band at 452 nm disappears within 4 h due to decay of **3** to **4**, the latter being insoluble in acetone. The formation of **3** in acetone was observed to occur already at low temperatures (approximately -70°C), albeit at very low rates. Quantitative conversion of **1** to **3** was observed at ca. -40°C . At this temperature, **3** is stable for several hours in solution and can be isolated by precipitation with cold diethyl ether with the resulting orange solid being stable at -30°C for some days.

EPR spectroscopy:

EPR studies were carried out in order to investigate the composition of **3**. Paramagnetic, oxygen-free compound **2** displays a singlet signal at $g = 2.10$ in acetone.⁸ Due to their diamagnetic nature, complex **1** and *in situ* generated compound **3** do not show any EPR activity in acetone, with the exception of a small EPR signal arising from minor decomposition of **3** to **2**.⁸ To confirm the presence of an iron-bound superoxide, 5,5-Dimethyl-1-pyrroline *N*-oxide (DMPO) was utilized as superoxide trapping reagent. Oxygen centered radicals can react with DMPO to form EPR active oxidation products.¹⁷ A blank experiment using pure DMPO did not show any EPR activity (Figure 3, left). After the reaction of **2** with DMPO under inert gas, a triplet signal with a $g = 1.97$ (Figure 3, left) was observed, whereas the signal at $g = 2.10$ (relative to pure **2**) disappeared. To a minor extent, this signal was also found for **1** in the presence of DMPO, most likely arising from partial oxidation of **1** to **2** by the *N*-oxide. If **2** was reacted with DMPO in the presence of O_2 ; no difference with the oxygen-free reaction could be observed for **2**+DMPO+ O_2 ($g = 1.97$), as Fe(III) cannot reduce molecular oxygen. For **1**+DMPO+ O_2 a triplet signal with $g = 1.95$ was obtained (Figure 3, middle).¹⁸

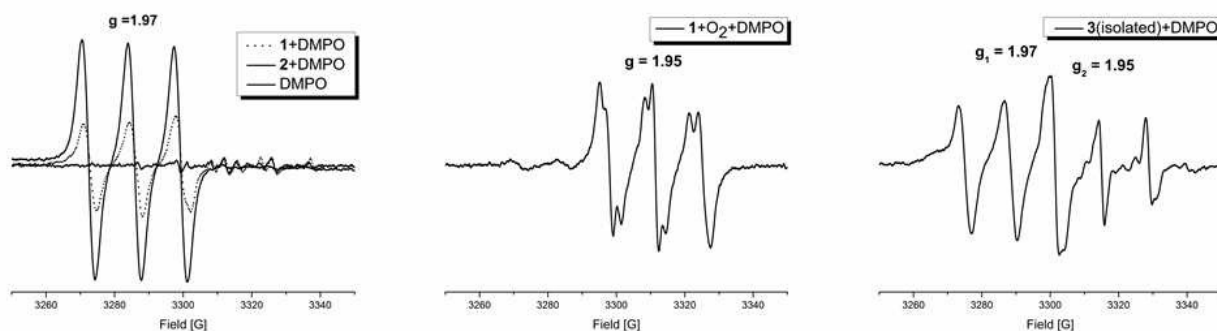


Figure 3. X-band EPR spectra (298 K) in acetone of: pure DMPO, **1**+DMPO and **2**+DMPO under an inert atmosphere (left), **1**+DMPO in the presence of oxygen (middle) and of isolated **3**+DMPO (right).



Journal Name

ARTICLE

Finally, the reaction of isolated **3** with DMPO under an inert atmosphere gives rise to two independent signals with $g = 1.97$ and $g = 1.95$ (Figure 3, right). The signal at $g = 1.95$ correlates to that found for **1**+DMPO+O₂, whereas the signal at $g = 1.97$ is identical to that observed upon reaction of Fe(III) species complex **2** with DMPO under inert atmosphere (as well as in the presence of O₂) and hints at a partial decomposition of **3** to complex **2** under the reaction conditions. These experiments suggest that **3** should contain the same kind of oxygen centered radical formed upon reaction of **1** and O₂. As the reaction of **3**+DMPO was performed under an inert gas atmosphere, the oxygen radical should be bound to the Fe center of compound **3**. These findings strongly support the proposed superoxidic nature of species **3**.

¹H-NMR studies:

Compound **3** is diamagnetic and therefore suitable for ¹H NMR investigations (see Figures S2, S4 and S5 in the ESI). The diamagnetic nature of **3** can be explained by the antiferromagnetic coupling of the unpaired electrons on the Fe(III) center and the O₂⁻ ligand.^{3a,19} In agreement with the structure obtained from density functional theory (DFT) studies (Figure 4) the ¹H NMR of **3** does not indicate coordinating acetonitrile ligands. The CH₂ bridges of the backbone of **3** display signals at 6.48 ppm and 6.31 ppm. The splitting (²J_{HH} = 13.1 Hz) observed suggests a square pyramidal geometry for **3** that is similar to the nitrosyl derivative of **1** that has been previously described by our group.⁷ A fast fluxional behavior between side-on and end-on coordination of the O₂⁻ on an NMR scale cannot be excluded. The suggested side-on coordination of the superoxide is based on DFT calculations.

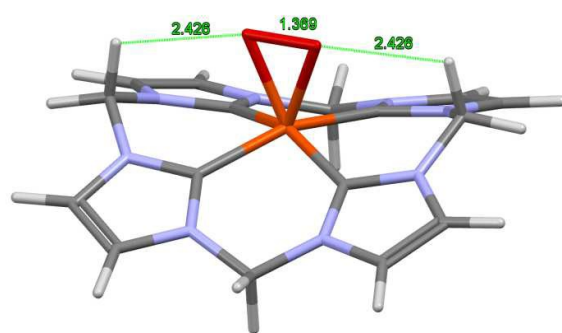


Figure 4. DFT-derived structure of the cationic fragment [Fe(O₂)CCCC]²⁺ of **3**. Selected calculated bond lengths (Å) and angles (°): Fe1-C1: 1.966, Fe1-C5: 1.956, Fe1-O1: 1.883, O1-O1*: 1.369, O1-H8: 2.426, C1-Fe1-C5: 87.62, C5-Fe1-C9: 89.73, O1-Fe-O1*: 42.63, C8-H8-O1: 105.79.

A valid energetic minimum for the geometry optimization was obtained only in case of side-on coordination of the superoxide and the respective square pyramidal geometry with a calculated O–O bond length of 1.369 Å. This value confirms the expected lengthening of the dioxygen bond upon coordination (free O₂: 1.21 Å/ free O₂⁻: 1.33 Å).²⁰ Interestingly, an interaction between the oxygen atoms and two of the protons of the CH₂ bridges is indicated with O–H distances of 2.43 Å, suggesting a stabilizing effect on **3**. Comparable observations were made by various groups reporting on molecular structures of Fe(IV) oxo complexes, where O–H interactions with similar distances were revealed.^{11,21} ¹H NMR kinetics of the formation and decay of **3** in acetone are in agreement with the UV/Vis experiments (Figure 5, see also Section 5 of the ESI). After exposing a solution of **1** in acetone-d₆ to O₂ at -40 °C, rapid formation of the characteristic signals of **3** (6.48 ppm and 6.31 ppm) is observed, while the signals of **1** (7.86 ppm, 6.63 ppm and of Fe-coordinated MeCN at 1.7 ppm) decrease. After 3 h at -40 °C a mixture of 31 % **1** and 43 % **3** - relative to the initial amount of **1** - is obtained whereas the remaining 26 % precipitate as the blue compound **4**. Allowing the reaction to warm up to 25 °C within 40 min leads to complete conversion to **3** and its simultaneous decomposition to **4**. Complete conversion of **1** is observed at -10 °C with a maximum yield of 68 % of **3**. At temperatures above -10 °C, **3** readily decomposes to **4** within less than 1 h. At the end of the experiment a blue solid precipitated. This precipitate could be identified as pure **4** by means of ¹H-NMR spectroscopy in CD₃CN.

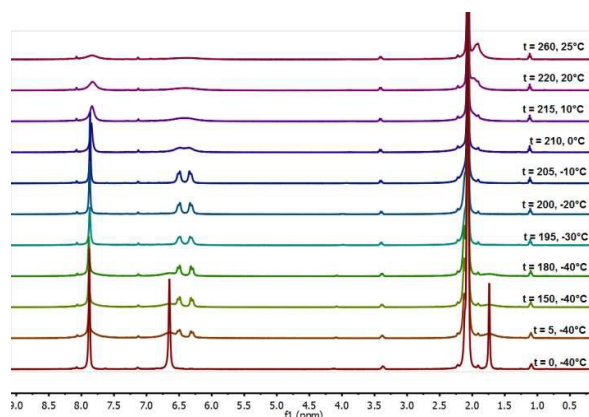


Figure 5. Formation of **3** from **1** and O₂ and subsequent decay of **3** to **4**, monitored by ¹H NMR in acetone-d₆. (1 bar O₂, T = -40°C to 25 °C, [1]₀ = 1 • 10⁻³ M).

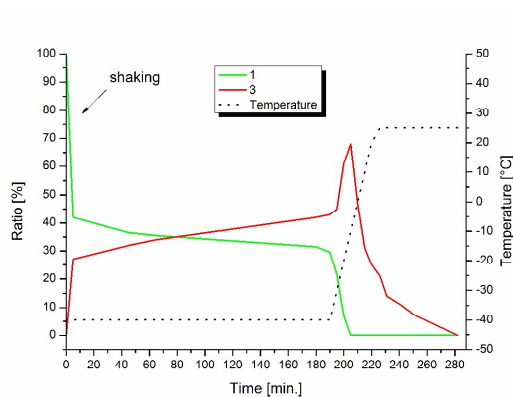
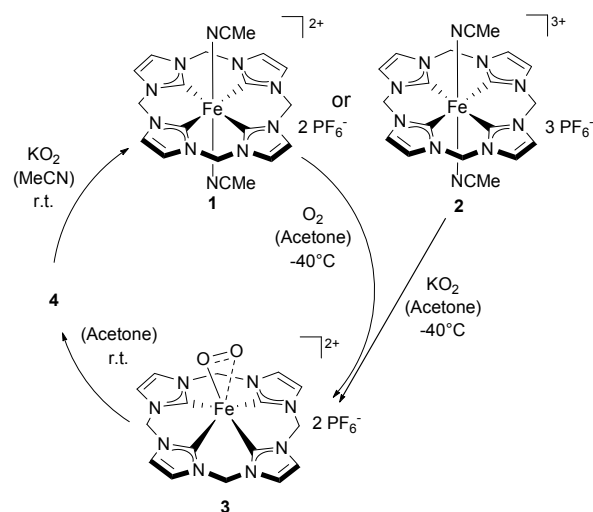


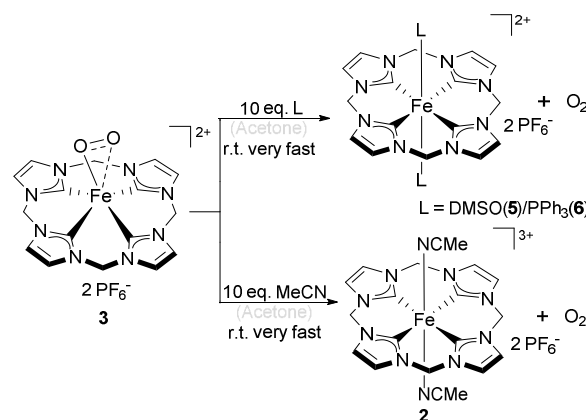
Figure 6. Formation and decay of **3** (red) from **1** (orange) and O₂ in acetone, monitored by ¹H NMR based on the integration of the signals at 7.85 (**1+3**), 6.59 (**1**) and 6.31 (**3**) ppm (internal standard Et₂O). (1 bar O₂, T = -40°C to 25°C, [1]₀ = 1•10⁻³ M).

Reactivity studies on **3**:

As **3** can be generated in acetone from **1** (Scheme 2) it appears reasonable to assume that **3** can also be formed by the reaction of **2** with KO₂ at temperatures from -80 °C to 25 °C by ¹H NMR confirms the suggested reaction pathway (for details and spectra see Figure S7 in the ESI). Upon warming from -80°C to -40°C complete conversion of **2** to **3** was observed in the presence of KO₂. Once again, a further increase in temperature up to r.t. leads to the disappearance of all ¹H-NMR signals and to the precipitation of **4** as a dark blue solid. **4** could be reduced to **1** in acetonitrile by addition of KO₂, thus closing the ideal redox circle. Therefore, O₂⁻ may serve as a reducing agent for Fe(III) compounds (**2** and **4**), whereas O₂ acts as an oxidant for Fe(II) complex **1**. Dimeric Fe(III)-O-O-Fe(III) compounds have been reported to be paramagnetic and to be irreversibly formed from oxygen and Fe(II) precursors.¹⁴



Scheme 3. Reactivity of **1** with O₂ or **2** with KO₂ in acetone affording **3** at -40 °C and subsequently **4** after warming. **4** can be converted to **1** by reaction with KO₂ thus ideally closing a reversible redox cycle of **1**.



Scheme 4. Reactivity of **3** with PPh₃, DMSO, and MeCN in acetone.

Compound **3** however, is diamagnetic and it can be reversibly converted to an Fe(II) complex analogous to **1** by addition of more nucleophilic ligands such as PPh₃ or DMSO in acetone (Scheme 4). PPh₃ and DMSO are not oxidized during this process, behaving exclusively as displacing ligands under formation of **5** or **6** (see Figure S6 in the ESI). The addition of acetonitrile (10 equiv.) in acetone leads to the formation of complex **2** (compare with Scheme 3). This is in good agreement with previous reports on superoxo species²² and with the observed reactivity between of **1** and O₂ in acetonitrile leading to complex **2**.

Preparation and characterization of **4**:

Complex **4** was prepared in high purity by adding oxygen to a concentrated acetone solution of **1** (>50 mM) at -40°C followed by slow warming to r.t.. Product formation was indicated by the precipitation of a dark blue powder in good yields (60-70%). Instead of acetone also benzonitrile or pivalonitrile as solvents afforded good yields of **4**. Additionally **4** could also be prepared by using air instead of dry oxygen at r.t., albeit in significantly lower yields (~10%). Both Fe(III) centers in **4** formally consist of 15 valence electrons; nevertheless, **4** is diamagnetic and therefore suitable for NMR-spectroscopy. This is attributed to antiferromagnetic coupling of the unpaired electrons over the bridging oxide, which is known for similar systems.¹¹ In ¹H NMR a singlet at 7.57 ppm is observed for **4**. In addition, two doublets of the bridging CH₂ groups with geminal couplings of 13.1 Hz arise at 6.08 and 5.94 ppm. The ¹³C NMR spectrum of **4** shows two sharp signals at 122.72 and 64.05 ppm, which are assigned to the backbone CH groups and the CH₂ bridges, respectively. The signal of the coordinating carbons only appears as a broad peak at 175 ppm. Slow diffusion of oxygen-enriched diethyl ether into an acetone solution of **1** allowed collection of single crystals of **4** suitable for single crystal X-ray diffraction (SC-XRD, Figure 7). The molecular structure shows a slightly distorted square pyramidal geometry with the tetradentate cyclic ligand coordinated in saddle distorted fashion. The Fe-C_{NHC} distances of **4** with its saddle-distorted ligand

ARTICLE

Journal Name

conformation average to 1.949 Å, which is slightly shorter than for comparable Fe(III)OFe(III) tetracarbene complexes (~1.99 Å) reported by Meyer et al.¹¹ The Fe-O distance is 1.732 Å and the FeOFe angle is 162.7°.

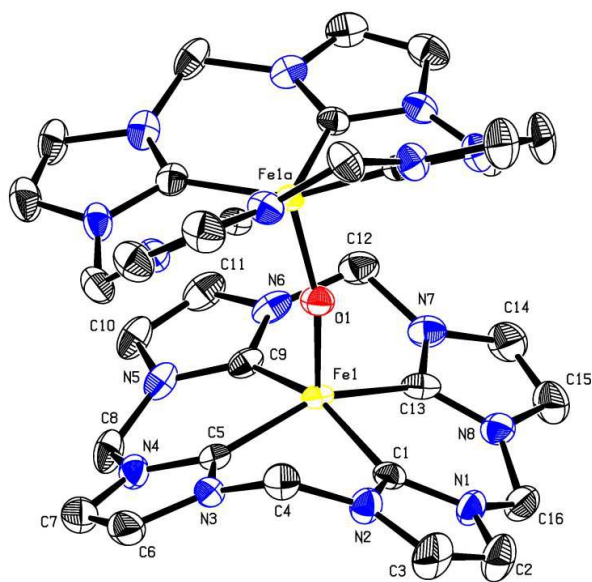


Figure 7. Ortep-style drawing of the cationic fragment of $O[Fe(III)CCCC]_2^{4+}$ of **4**. Hydrogen atoms and PF_6^- anions are omitted for clarity and thermal ellipsoids are shown at a 50% probability level. Selected bond lengths (Å) and angles (°): Fe1–C1: 1.948(4), Fe1–C5: 1.941(1), Fe1–C9: 1.943(4), Fe1–C13: 1.966(4), Fe1–O1: 1.7322(7), C1–Fe1–C5: 87.28(16), C5–Fe1–C9: 87.84(17), C9–Fe1–C13: 87.20(17), C1–Fe1–N13: 86.92(16), C1–Fe1–O1: 101.55(16), C5–Fe1–O1: 100.80(12), C9–Fe1–O1: 102.30(16), C13–Fe1–O1: 105.47(12), Fe1–O1–Fe1a: 162.7(2).

Reactivity of **4**:

Compound **4** is able to act as an oxidizing agent. For instance, PPh_3 is stoichiometrically oxidized to $OPPh_3$ (Scheme 5) under formation of **1** (see the ESI). Reduction of **4** to **1** is observed in the presence of reducing agents such as Zn powder, Fe-powder, hydroquinone (H_2Q), or KO_2 . At r. t. in CD_3CN one third of the initial amount of **4** is reduced to **1** after approximately 5 d. (see Figure S9 in the ESI). As reported for the case of the oxidation of **1** to **2** by oxygen in acetonitrile, oxidation products cannot be observed by 1H - or 2D -NMR. In the absence of other reducing agents, very slow oxidation of acetonitrile by **4** is observed at r.t.. Upon heating an acetonitrile solution of **4** to reflux, full conversion to **1** takes place within 5 min. Furthermore, **4** can also be deoxygenated to quantitatively yield **2** by the simple addition of stoichiometric amounts of strong Brønsted acids (e.g. HBF_4/HPF_6) at r.t..

Conclusions

The reactivity of an heme analogue Fe(II) (**1**) compound with molecular oxygen was investigated and three different Fe(III) compounds, have been identified and characterized. In their structural characteristics, all of them are closely related to heme systems. A strong influence of the solvent

on the reactivity is observed, resulting in two different products from the oxidation of **1** with molecular oxygen: The oxide bridged Fe(III) dimer **4** in acetone and the metheme like Fe(III) complex **2** in acetonitrile. The intermediate proposed in both cases, the Fe(III) superoxide (**3**), as well as the oxide bridged Fe(III)dimer (**4**) have been studied. Indirect chemical and spectroscopic evidence (EPR spin trap experiments, NMR spectroscopy) of the superoxidic nature of **3** has been presented. **3** is prone to ligand exchange reactions, resulting in reductive dissociation of dioxygen upon addition of nucleophilic ligands such as PPh_3 and DMSO. In the latter case the oxide bridged Fe(III) dimer **4** acts as an oxidant while being reduced to **1**. Also, **4** can be deoxygenated under the retention of its formal oxidation state to yield **2**. With respect to iron-based systems in nature, which are widely used as oxidation catalysts, oxygen activation by artificial systems is of high interest. A deeper understanding of the reactivity of such complexes can help to improve the quality of artificial, bio-inspired iron systems for various applications.

Acknowledgements

M.R.A. and S.H. gratefully acknowledge support by the TUM Graduate School. This project was supported through a collaboration with the King Abdullah University of Saudi-Arabia (Grant No. KSA-C0069/UKC0020).

Notes and references

- (a) W. Nam, *Acc. Chem. Res.*, 2015, **48**, 2415; (b) Y. You and W. Nam, *Chem. Sci.*, 2014, **5**, 4123; (c) P. C. A. Bruijninx, G. van Koten and R. J. M. Klein Gebbink, *Chem. Soc. Rev.*, 2008, **37**, 2716; (d) H. Chen, M. Ikeda-Saito and S. Shaik, *J. Am. Chem. Soc.*, 2008, **130**, 14778; (e) E. G. Kovaleva, M. B. Neibergall, S. Chakrabarty and J. D. Lipscomb, *Acc. Chem. Res.*, 2007, **40**, 475; (f) S. V. Kryatov, E. V. Rybak-Akimova and S. Schindler, *Chem. Rev.*, 2005, **105**, 2175.
- (a) K. Ray, F. F. Pfaff, B. Wang and W. Nam, *J. Am. Chem. Soc.*, 2014, **136**, 13942; (b) S. P. de Visser, J. H. Rohde, Y.-M. Lee, J. Cho, and W. Nam, *Coord. Chem. Rev.*, 2013, **257**, 381; (c) D. Mandon, H. Jaafar and A. Thibon, *New J. Chem.*, 2011, **35**, 1986; (d) W. A. van der Donk, C. Krebs and J. M. Bollinger Jr., *Curr. Opin. Struct. Biol.*, 2010, **20**, 673; (e) G. Dong, S. Shaik, W. Lai, S. P. de Visser, S. Shaik and W. Nam, *Chem. Commun.*, 2012, **48**,

- 2189; (g) R. Latifi, L. Tahsini, W. Nam and S. P. de Visser, *Phys. Chem. Chem. Phys.*, 2012, **14**, 2518; (h) F. Bonnot, T. Molle, S. Ménage, Y. Moreau, S. Duval, V. Favaudon, C. Houée-Levin and V. Nivière, *J. Am. Chem. Soc.*, 2012, **134**, 5120; (i) H. Chen, K.-B. Cho, W. Lai, W. Nam and S. Shaik, *J. Chem. Theory Comput.*, 2012, **8**, 915; (j) L. W. Chung, X. Li, H. Hirao and K. Morokuma, *J. Am. Chem. Soc.*, 2011, **133**, 20076.
- 3 (a) F. Oddon, Y. Chiba, J. Nakazawa, T. Ohta, T. Ogura and S. Hikichi, *Angew. Chem. Int. Ed.*, 2015, **54**, 7336; (b) C.-W. Chiang, S. T. Kleespies, H. D. Stout, K. K. Meier, P. Y. Li, E. L. Bominaar, L. Que Jr., E. Münck and W.-Z. Lee, *J. Am. Chem. Soc.*, 2014, **136**, 10846.
- 4 (a) M. M. Mbughuni, M. Chakrabarti, J. A. Hayden, E. L. Bominaar, M. P. Hendrich, E. Münck and J. D. Lipscomb, *Proc. Natl. Acad. Sci. U.S.A.*, 2010, **107**, 16788; (b) C. Costentin, H. Dridi and J.-M. Savéant, *J. Am. Chem. Soc.*, 2015, **137**, 13535; (c) K. Duerr, O. Troeppner, J. Olah, J. Li, A. Zahl, T. Drewello, N. Jux, J. N. Harvey and I. Ivanović-Burmazović, *Dalton Trans.*, 2012, **41**, 546; (d) W. Xu, K. Dziedzic-Kocurek, M. Yu, Z. Wu and A. Marcelli, *RSC Adv.*, 2014, **4**, 46399.
- 5 (a) J.-H. Jeoung, M. Bommer, T.-Y. Lin, H. Dobbek, *Proc. Natl. Acad. Sci. U.S.A.*, 2013, **110**, 12625; (b) Kovaleva, E. G.; Lipscomb, J. D. *Science*, 2007, **316**, 453.
- 6 S. Hong, K. D. Sutherlin, J. Park, E. Kwon, M. A. Siegler, E. I. Solomon and W. Nam, *Nat. Commun.*, 2015, **5**, 5440.
- 7 M. R. Anneser, S. Haslinger, A. Pöthig, M. Cokoja, J. M. Basset and F. E. Kühn, *Inorg. Chem.*, 2015, **54**, 3797.
- 8 J. W. Kück, M. R. Anneser, B. Hofmann, A. Pöthig, M. Cokoja and F. E. Kühn, *manuscript under revision*.
- 9 (a) J. W. Kück, A. Raba, I. I. E. Markovits, M. Cokoja and F. E. Kühn, *ChemCatChem*, 2014, **6**, 1882; (b) A. Raba, M. Cokoja, W. A. Herrmann and F. E. Kühn, *Chem. Commun.*, 2014, **50**, 11454; (c) S. Haslinger, A. Raba, M. Cokoja, A. Pöthig and F. E. Kühn, *J. Catal.*, 2015, DOI: 10.1016/j.jcat.2015.08.026.
- 10 (a) I. V. Korendovych, O. P. Kryatova, W. M. Reiff and E. V. Rybak-Akimova, *Inorg. Chem.*, 2007, **46**, 4197; (b) D. J. Liston and B. O. West, *Inorg. Chem.*, 1985, **24**, 1568; (c) D.-H. Chin, N. Gerd, G. N. La Mar and A. N. Balch, *J. Am. Chem. Soc.*, 1980, **102**, 4344.
- 11 S. Meyer, I. Klawitter, S. Demeshko, E. Bill and F. Meyer, *Angew. Chem. Int. Ed.*, 2013, **52**, 901.
- 12 J. Umbreit, *Am. J. Hematol.*, 2007, **82**, 134.
- 13 I. Klawitter, M. R. Anneser, S. Dechert, S. Meyer, S. Demeshko, S. Haslinger, A. Pöthig, F. E. Kühn and F. Meyer, *Organometallics*, 2015, **34**, 2819.
- 14 C. E. Tinberg and S. J. Lippard, *Biochemistry*, 2010, **49**, 7902.
- 15 D. E. Feirman and A. I. Cederbaum, *Chem. Res. Toxicol.*, 1989, **2**, 359.
- 16 T. Foo and A. Panova, Process for the Synthesis of Glycolonitrile, US 7368492, May 6, 2008.
- 17 (a) R. Lia, H. Kobayashi, X. Yana and J. Fan, *Catal. Today*, 2014, **233**, 140; (b) J.-L. Clement, N. Ferre', D. Siri, H. Karoui, A. Rockenbauer and P. Tordo, *J. Org. Chem.*, 2005, **70**, 1198; (c) G. R. Buettner, *Free Rad. Res. Comms.*, 1993, **19**, 79.
- 18 Z. Barbierikova, M. Mihalikova and V. Brezova, *Photochem. Photobiol.*, 2012, **88**, 1442.
- 19 J. P. Collman, C. J. Sunderland, K. E. Berg, M. A. Vance and E. I. Solomon, *J. Am. Chem. Soc.*, 2003, **125**, 6648.
- 20 *CRC Handbook of Chemistry & Physics*, Ed. D. R. Lide, Taylor and Francis, 90th Edition, 2009.
- 21 J. Li, B. C. Noll, A. G. Oliver, C. E. Schulz and W. R. Scheidt, *J. Am. Chem. Soc.*, 2013, **135**, 15627.
- 22 P. L. Holland, *Dalton Trans.*, 2010, **39**, 5415.

Textual Abstract:

The reactivity of an heme-like organometallic Fe NHC complex with molecular oxygen is investigated and the formation of a superoxo Fe(III) intermediate is observed. Further the reactivity of the intermediate in acetone and acetonitrile is described and the respective final products are identified.

Graphical Abstract:

